# CHAPTER 4

# Micro-Doppler Signature Based Moving Target Classification*




*Part of this work has been published as:

**Vineet Singh**, Somak Bhattacharyya, and Pradip Kumar Jain, "Micro-Doppler classification of human movements using spectrogram spatial features and support vector machine," *International Journal of RF and Microwave Computer-Aided Engineering,* vol. 30, no. 8, p. e22264, 2020.

# CHAPTER 4

# Micro-Doppler Signature Based Moving Target Classification

In previous chapters applications of the wideband ranging system in target localization and life sign characteristic determination have been investigated. In *Chapter 3*, it has been observed that when a person remains in rest his physiological properties can be used to detect his presence. However, when the target is non-stationary, i. e. the position or orientation of the target is continuously changing, then the discussed moving target indictor (MTI) processing based scheme fails to retrieve the target information. In the present chapter, *Chapter 4*, incorporates a narrow-band radar-based method for obtaining target information that exists due to the movement of main-body and structural components based on the concept of continuous wave (CW) Doppler radar.

In this chapter, the close human movement activities classification is carried out for five distinguished activities with the help of CW radar captured data involving the advantage of the spatial features. In this study, five distinguished human activities are taken into consideration for the purpose of classification viz., (i) walking and pushing an object (a chair), (ii) standing and swinging both the arms, (iii) walking with no hand swing (holding a smaller object with both hands), (iv) standing and swinging single arm (right hand) only, and (v) normal walking. For the training of the classifiers, training features have been defined on the basis of texture analysis of the spectrogram. In order to perform texture analysis, statistical methods are utilized considering each pixel value of information available in the spectrogram image. Thus, the human intervention for feature generation undergoes reduction. In order to predict the movement activity class, support vector machine (SVM) classifiers are trained in one versus all (OVA) configurations. The adopted method of human activities classification involves the least feature extraction complexity and provides a very high cross validation and prediction accuracy hence can be used at the surveillance sites for more reliable results.

The Doppler modulation frequencies caused by a moving target are determined by the carrier frequency, the velocities, and the angles between the direction of motion and path of the transmitted and reflected radar signals [Dave 2015]. For a simple point scatterer moving with a speed *v* with respect to a stationary transceiver system, the Dopplers shift $f_d$ can be given as:

$$f_d = f_t \frac{v}{c}(\cos\theta_i + \cos\theta_o) \quad , \tag{4.1}$$

where $f_t$ is the transmitted signal frequency, *c* is the speed of light in the medium, $\theta_i$ is the angle between the target velocity and the incoming wave, while $\theta_0$ is the angle formed by the target velocity and the reflected wave. For a monolithic system, the expression $\theta_i \simeq \theta_o$ and the Doppler shift expression can be approximated as:

$$f_d = 2f_t \frac{v}{c}(\cos\theta_i) \quad . \tag{4.2}$$

For complex targets, such as walking human, the velocity of each body parts varies with time. For a certain observation time duration, the radar cross-section (RCS) of different parts of the body is also a function of aspect angles and transmitted frequencies. These structural components on the body often have complex motions, called micro motions, such as vibration, rotation, or acceleration in addition to the translation, which follows a unique repetitive pattern of motion with time. The Doppler analysis of radar returns from such a complex target will show a band of Doppler frequency shift around a main bulk Doppler which vary with time and often termed as micro-Dopplers [Chen *et al.* (2006), Thayaparan *et al.* (2008)]. Due to their stability and distinguishability, micro-Doppler characteristics can be considered as a unique signature of a target [Chen *et al.* (2006)].

## 4.1 Human Activity Classification Methodology

The task of object movement classification into different groups involve three main phases, as shown in Figure 4.1. The first phase is input data preparation, followed by the second phase involving feature extraction from the captured data. Then, the final and third phase is the classification of human activities using the identified features [Fioranelli *et al.* (2015), DU *et al*. (2016), DU *et al.* (2014), Shi *et al*. (2015)]. The first and second phases are necessary for both times, i.e., for the training of the classifier as well as prediction of the class labels. In the classification stage, some portion of the extracted features are used to train the classification model while the remaining part is deployed for predicting the activity class. All the mentioned phases are the combination of processing steps as shown in Figure 4.2 and explained here in details.

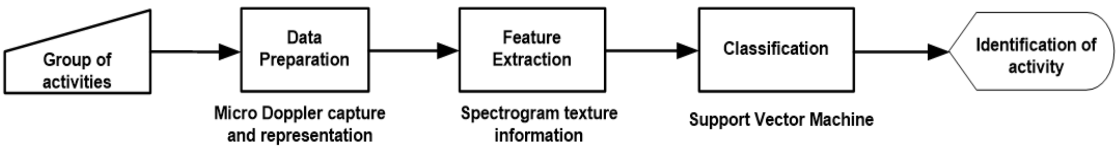


**Figure 4.1:** Micro-Doppler classification process.

In the data generation phase, the data collection is required corresponding to each activity. A CW radar is synthesized in laboratory to capture the real time micro-Doppler information generated through the test human subjects performing different typical movements. The developed system is coherent in nature and records the time domain reflection coefficient in the complex form and stores the In-phase and Quadrature-phase (I-Q) components for a fixed time span at certain sampling interval. Before going for the joint time frequency analysis, a preprocessing is done where the mean of the individual time domain data is subtracted out in order to remove the signal level mismatch. Since it is equivalent to constant term subtraction, it does not affect the frequency content of the signal. The collected data is represented in the form of spectrogram images with the help of short time Fourier transforms (STFT). The 5.0 second duration signal for each experimental data contains total 5000 samples in length. The selected time window length and overlap have been chosen as 0.30 second and 0.28 second, respectively, for the calculation of short time Fourier transform which satisfies both the time and frequency domains resolution simultaneously. The micro-Doppler signatures contained in a spectrogram are highlighted using background clipping where the clipping threshold is decided by the spectrogram texture statistics. The second phase defines texture features on the complete signature highlighted spectrogram image using statistical parameters. For all the data, extracted features are arranged and fed to the classification phase. The classification phase involves a Support Vector Machine (SVM) classifier which receives feature sets as an input out of which 80% are used for model training while the remaining 20% are used for predicting the actual class labels of the activities, as depicted from Figure 4.2. The binary SVM classifiers are used in one versus all (OVA) configuration for the classification of five different activity classes. During training of the SVM classification model, five-fold cross validation is used to predict the classifier's training response on the testing data.

## 4.2 Experimentation and Data Collection

To implement the adopted methodology (Figure 4.2), the CW radar is created in the laboratory. The experimental setup scheme and data collection procedure is briefly described below.

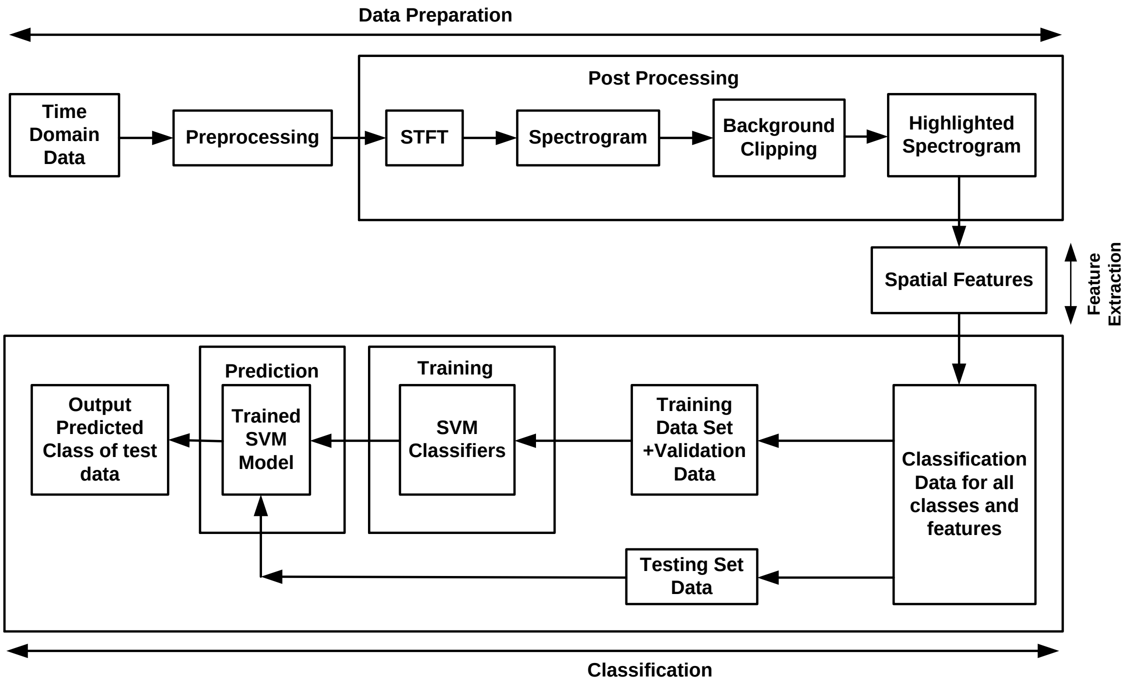


**Figure 4.2:** Adopted methodology.

### 4.2.1 Experimental Setup

For experimental setup synthesis in the laboratory, a performance network analyzer (PNA) Agilent N5222A is used to work as a coherent, CW radar source. For transmission and reception purpose of the electromagnetic waves in the medium, two dual-ridge horn antennas are used. The antennas are connected to the two ports of the PNA using coaxial cables and placed in a common vertical plane and a transceiver system is designed as shown in Figure 4.3(a). The synthesized system contains a higher sampling rate of 1000 samples per second with measurement ability of two quadrature-phase components I and Q format of the data. The created system is capable to record the back scattered signals in the form of reflection coefficient viz., $S_{21}$ in the time domain with higher signal to noise ratio (SNR) value. All the experiments are performed at a CW frequency of 6.5 GHz. The other specifications and details are provided in Table 4.1.

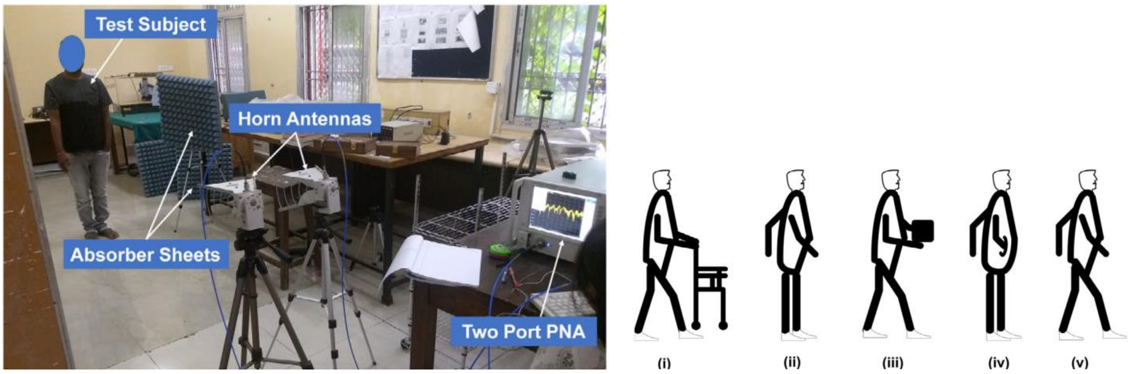


**(a)** **(b)**

**Figure 4.3:** (a) Experimental setup synthesized for micro- Doppler experiments; (b) Five different human movement classes under consideration of the experiment.

**Table 4.1:** Experimental setup details.

| **Sr. No.** | **Parameter/ Type** | **Value/ Specification** |
|---|---|---|
| 1. | Source | Agilent PNA N5222A |
| 2. | Antenna | Dual ridge AmitecDRH20 |
| 3. | Operating CW Frequency | 6.5 GHz |
| 4. | Data type | $S_{21}$ |
| 5. | Observation time for each experiment | 5 seconds |
| 6. | Sampling frequency | 1 KHz |
| 7. | Joint time-frequency analysis method | Short time-frequency analysis (STFT) |
| 8. | Transmitted power | 0 dBm |

### 4.2.2 Experimental Data Collection

The developed system is utilized for the measurement of different movements performed by test human subjects. In this work, five practically possible human activities that may occur at the security observation cite has been considered for the classification, and accordingly the data are collected for these classes in the laboratory. These five classes involve the walking and pushing some object (chair is pushed towards the radar), swinging arms while standing at the same place, walk and no arm swing (case of holding some object using both hands), swing of single (right) arm standing at the same place and normal walk of a person. The vector diagrams of the considered cases are shown in Figure 4.3(b). Although this study can also be further extended for more possible data classes to test the proposed method's classification capability for distinguishing very close classes, only these five experimental cases are selected here for the micro-Doppler classification. The antenna height is fixed at 1.2 m above the ground. The radar antenna has been tilted in such a way that out of these five experimental classes, three cases of walking of human subject remains in the field of view of antenna for a maximum time of the walk. To ensure the suppression of Doppler noise in the field of view of antenna, a few microwave absorber sheets have been used. To make the general data, three persons with different physique are selected for performing such activities in which each of them performed 10 activities for each of the experiment class. Henceforth for each class of data, 30 separate experimental data are acquired and total 150-time domain data are captured for all the five classes. The data capture time is selected as 5.0 seconds for all the classes. Experiments including walking have approximately seven steps covered by the test subjects. In hand swing cases, the location of the test subjects is altered for data collection to create the range variations; thereby creating a condition for practical application.

## 4.3 Spectrogram Spatial Feature

Feature extraction from the data is a necessary phase of moving target classification. The proposed human movement activity classification method is based on the spatial feature extraction of spectrogram. The concept of generation of the spectrogram from time domain data and extracted spatial features are described in this section.

### 4.3.1 Micro-Doppler Spectrogram

In most cases, due to complex relative motions between radar and targets, the frequency spectrum of radar returns are time-varying in nature. Frequency components present in the radar received signal contains the velocity information of subjects. The Fourier transform is one of the conventional and popular methods for frequency analysis. Still, for long time duration and real time-varying signals, it fails to provide the time-dependent frequency information, e. g., music signal audio signal, radar return, etc. Joint time-frequency transforms were developed for the frequency analysis of real time-varying signals like STFT, Wigner valley, Wavelet, etc. [Chen *et al*. (2006), Chen and Ling (2002)]. The simpler and widely accepted time-frequency transform is STFT, where a moving time window slides over the complete length of time-domain data, and Fourier transform is evaluated for each of the window position [Chen and Ling (2002), Tivive *et al.* (2010)]. If *S(n)* is a time varying sampled signal at time instant *n*, then the STFT generated spectrogram *S(n, f)* can be given by:

$$S(n,f)=\left|\sum S(n)W(n-k)\exp(-j2\pi fn)\right|^{2} \quad . \tag{4.3}$$

Here, *n* and *k* are sample numbers while *W(n)* is window function. The resolution of the STFT spectrogram depends on the length of the window *n* [Chen and Ling (2002), Tivive *et al.* (2010), Shi *et al.* (2015)]. Increasing the time window length increases the frequency resolution and thereby reduces time axis resolution while decreasing of time window shows inverse effect [Chen and Ling (2002), Shi *et al.* (2015)]. The window functions are used to suppress the side lobes in the spectrogram which can be of different types such as Hamming, Hanning, Kaiser-Bessel, Gaussian, Blackman etc.[Chen and Ling (2002), Proakis and Manolakis (2014)]. In this work, Blackman window is selected in the processing due to its higher side lobe rejection and better accuracy behavior [Proakis and Manolakis (2014)].

### 4.3.2 Spatial Features Extraction

Image texture can be characterized as the spatial information contents recognized easily by human visuals [Materka and Strzelecki (1998)]. A texture can be physically considered as spatial arrangement of primitive having certain statistical regularity [Materka and Strzelecki (1998), Shi *et al.* (2015), Gonzalez and Woods (2002), Jähne (2005)]. The spectrogram of a non-stationary signal is an image where the intensity axis is signal strength, which is a function of time and frequency. Hence, the texture information of the micro-Doppler spectrogram can be analyzed quantitatively. Several methods exist for textural feature extractions. Statistical method is one of the popular and conventional method for the feature extraction.

The texture analysis of an image $R$ of dimension $M \times N$ is performed in which the intensity range of $R$ lies between [0, $L$-1] where $L$ is the number of possible intensity levels in the digital image. If $k_{th}$ intensity level is represented by $r_k$ and it occurs in the image for $n_k$ times; then the probability $p$ of occurrence of intensity level $r_k$ is given as [Gonzalez and Woods (2002)]:

$$p(r_k) = n_k / MN \quad . \tag{4.4}$$

By using equation (4.4), following image features are defined:

*Entropy*- The entropy of an image is the statistical measure of randomness that can be used to characterize the texture of any image. A spectrogram is energy distribution of frequency components with respect to time. For larger energy distribution a larger value of entropy is expected while for concentrated energy distribution a lower value of entropy is anticipated. The entropy $\varepsilon$ calculation can be carried out using the relationship [Gonzalez and Woods (2002)] given as:

$$\varepsilon = -\sum_{k=0}^{L-1} p(r_k)\log(p(r_k)) \quad . \tag{4.5}$$

*Mean*- The mean $\alpha_1$ is defined as the first moment around the zero for discrete distributions and it is equivalent to the measure of average intensity. The formula for the calculation of the mean can be given by [Gonzalez and Woods (2002)]:

$$\alpha_1 = \sum_{k=0}^{L} r_k\, p(r_k) \quad . \tag{4.6}$$

*Variance*- Variance $\alpha_2$ is a measure of spread out of a set of data. Zero variance value indicates that all of the data points are identical and lies over mean. On the other hand, the higher variance value infers that the data points are spread out from the mean position. The variance is expressed in (4.7), which shows that the average of the squared distance of each point to mean value [Gonzalez and Woods (2002), Jähne (2005)]:

$$\alpha_2 = \sum_{k=0}^{L} (r_k - \alpha_1)^2\, p(r_k) \quad . \tag{4.7}$$

*Skewness*- The asymmetry of a variable distribution is measured by the third moment of distribution and known as skewness $\alpha_3$. The zero skew value condition of a normal distribution indicates a symmetric distribution. A positive skew value indicates a longer right side tail than the left side of the distribution, and bulk of the values lies left to the mean. In contrast, a negative skewness indicates a longer left side tail than the right side of the distribution and bulk value remains right to the mean. Feature 4 is defined using skewness property of Doppler frequency strength distribution at each instant. To blend the skewness information of each time instant, an averaging is done and the mean skewness $\alpha_3$ can be defined as [Gonzalez and Woods (2002), Jähne (2005)]:

$$\alpha_3 = \frac{1}{N}\sum_{j=1}^{N}\sum_{k=0}^{L-1}(r_k - \alpha_1)^3 \, p(r_k) \quad , \tag{4.8}$$

where *j* is the number of time instants, i.e., number of columns of generated spectrogram, varying from 1 to *N*.

*Kurtosis*- The forth moment of distribution is known as kurtosis $\alpha_4$. It describes the collective weight of the tails with respect to the rest of the distribution. The value of kurtosis will be higher for the distribution with heavier tail. Feature 5 is defined based on Kurtosis and obtained for Doppler frequencies at each time instant and to merge all the M Kurtosis values averaging has been done with respect to number time instants. The expression for average kurtosis can be written as [Gonzalez and Woods (2002), Jähne (2005)] :

$$\alpha_4 = \frac{1}{N}\sum_{j=1}^{N}\sum_{k=0}^{L-1}(r_k - \alpha_1)^4 \, p(r_k) \quad . \tag{4.9}$$

## 4.4 Support Vector Machine

The classification as well as regression problems can be performed using Support vector machine (SVM) technique, a supervised machine learning algorithm. It is extensively used for many diverse classification problems owing to its superior performance over the state-of-the-art techniques viz., Fisher linear discriminator and the Bayesian decision method [Kim and Ling (2009)]. SVM has already been applied in the radar community for signal processing, radar target recognition, and micro-Doppler classification [Lei *et al.* (2011), DU *et al.* (2016), DU *et al.* (2014), Materka and Strzelecki (1998), Kim and Ling (2009)]. The basic aim of SVM is to define the optimal hyper-plane to distinguish the linearly separable data of two sets. Here, the optimal hyper-plane represents to the surface, which is not only used to separates the two sets of data but also come up with the largest margin between two classes, as illustrated in Figure 4.4(a). The optimal hyper-plane provides minimization of the generalization error of the classifier incorporating the feature data located on it [Lei *et al.* (2011)].

Accordingly, these feature data points are known as support vectors. In case of nonlinearly separable data, kernel tricks are utilized to solve nonlinear problems. Kernel functions are applied on each feature-data instance to map them into a space of higher-dimensions where they become linearly separable [Lei *et al.* (2011), Abe (2005)]. Thus, the optimal hyper plane of nonlinear feature-data could be found by SVM in a high-dimensional space in order to find the data classes. In our model, Gaussian Kernel function is used due to its versatile nature and no prior knowledge requirement about the data [Abe (2005)]. Scale factor of the Gaussian kernel function is crucial. Very high value of scale factor may lead to over-fitting and less generalization. On the contrary, extremely less value of it may lead to a constrained model too which can't capture the complexity or shape of the data and accordingly can behave as a linear kernel function. In this work, the scale factor of 1.00 has been chosen for the model training.

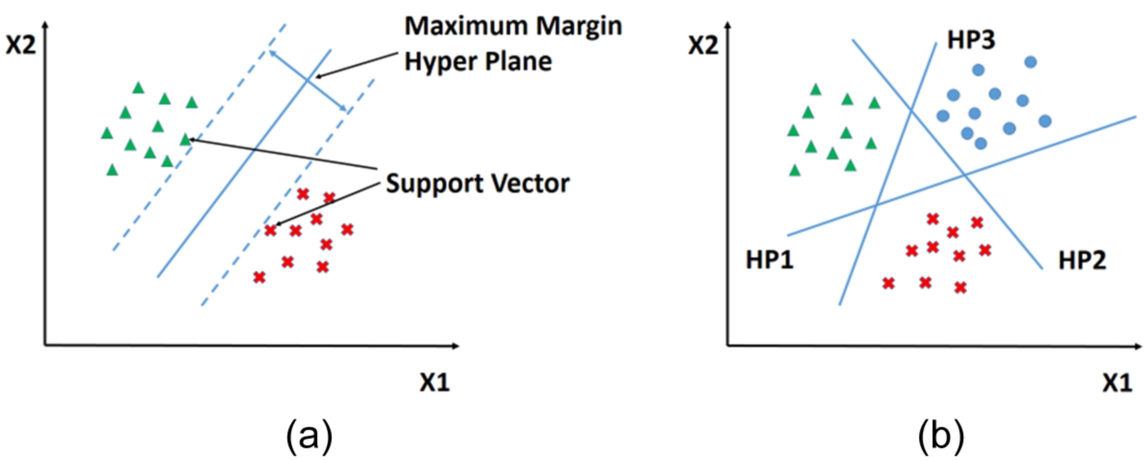


**Figure 4.4:** (a) Support vector machine hyper plane; (b) One versus all classification.

In our case, the data belong to five different classes leading to a multi-class classification problem for the present study. Two popular approaches exist in the world of Machine learning to incorporate the solution using SVM binary classifiers. The first approach is one versus one (OVO), while the second one is one versus all (OVA), which utilizes many binary classifiers. For the implementation of OVO for the multiclass problem, a decision tree structure is necessary while it requires the knowledge of class property. On the other hand, in OVA, the required N distinct binary classifiers for *N* classes of data and each classifier recognize a particular class as shown in Figure 4.4(b). OVA model is chosen in the multiclass classification, utilizing five distinct SVM classifiers.

## 4.5 Results and Discussion

In order to identify the type of human activity among the available typical activity classes, the synthesized CW radar system is used for recording of the data corresponding to different activities. Total 150 data are collected for five classes of human movement activities. The experimental data are labeled with number sequence ranging from 1 to 150. The data sequence belonging to each class label and type of experiment is listed in Table 4.2. Five different spatial texture features, as defined previously, are also computed from the spectrogram corresponding to each experimental data.

**Table 4.2:** Class belonging of data number.

| **Class label** | **Experiment name** | **Data number range** |
|---|---|---|
| **1** | Pushing chair with walk | 1-30 |
| **2** | Hand swing standing at fix position | 31-60 |
| **3** | Walking with no hand swing | 61-90 |
| **4** | Single hand swing standing at same position | 91-120 |
| **5** | Normal walk | 121-150 |

During the experiment the target is performing activities in a non-shield environment in order to create a practical scenario as shown in Figure 4.3 (a). The influence of reflections due to surrounding static obstacles will not affect the final classification accuracy since (a) they will remain common for all data; (b) the spread of these components are very less since they will appear in or around zero frequency line; (c) some of the features used in this work focuses on the spread of intensity which offer very less value in the classification dimension and results their minimum effect in the classification process."

All the five classes can be seen as the combination of two types of effects. Bulk motion which offers main Doppler and micro-Dopplers generated by movements of other subcomponents, like arms and leg swings. The bulk movements generate a highly concentrated energy distributions in joint time frequency plane while it is distributed for the objects generating micro-Doppler motions. The result generated at each phase of moving target classification has been obtained and covers the spectrogram generation, feature extraction and classification results.

### 4.5.1 Spectrogram Generation and Signature Highlighting

One of the spectrogram for all the five classes are shown after application of STFT in Figure 4.5 (a-d). We can observe that experiment classes, consisting of the movement of test subject towards the antenna, the received backscattered signal intensity increases with time. However, the activities performed while standing at some fixed locations (single and both hand swing experiments cases), the intensity remains unaltered for all the cycles, over a complete duration of data capture duration as depicted from Figure 4.5. For chair pushing case, the bulk Doppler is contributed primarily by chair's back support while small micro motion will be offered by the lower portion of the leg as significant portion of the body is covered by the vertical support of the chair. This is evident from Figure 4.5(a) where the bulk Doppler remains invariant with very low fluctuations along the

Doppler axis; resulting in appearance of small micro-Doppler around the bulk main-Doppler.

In hand swing case, sinusoidal type of variations involving symmetry is observed as shown in Figure 4.5(b). Figure 4.5(c) is associated with gait without hand swing where torso Doppler shows variation in frequency axis with respect to time increments due to the fact that the torso speed varies at different foot strikes of a walk cycle and offers a fluctuating bulk Doppler. In this case of experiment, the micro-Doppler frequencies can be observed with higher amount than the chair pushing case as the leg swing contribution in backscattered signal gets increased. The single hand swing at a fixed location produces a micro-Doppler signature provided in Figure 4.5(d) and can be seen as the half of the effect of both hand swing case. The case of Figure 4.5(e) involves the usual gait signature where a complex variation of limbs (hand swings and leg movements) generated micro-Doppler is also appearing on torso translation frequency.

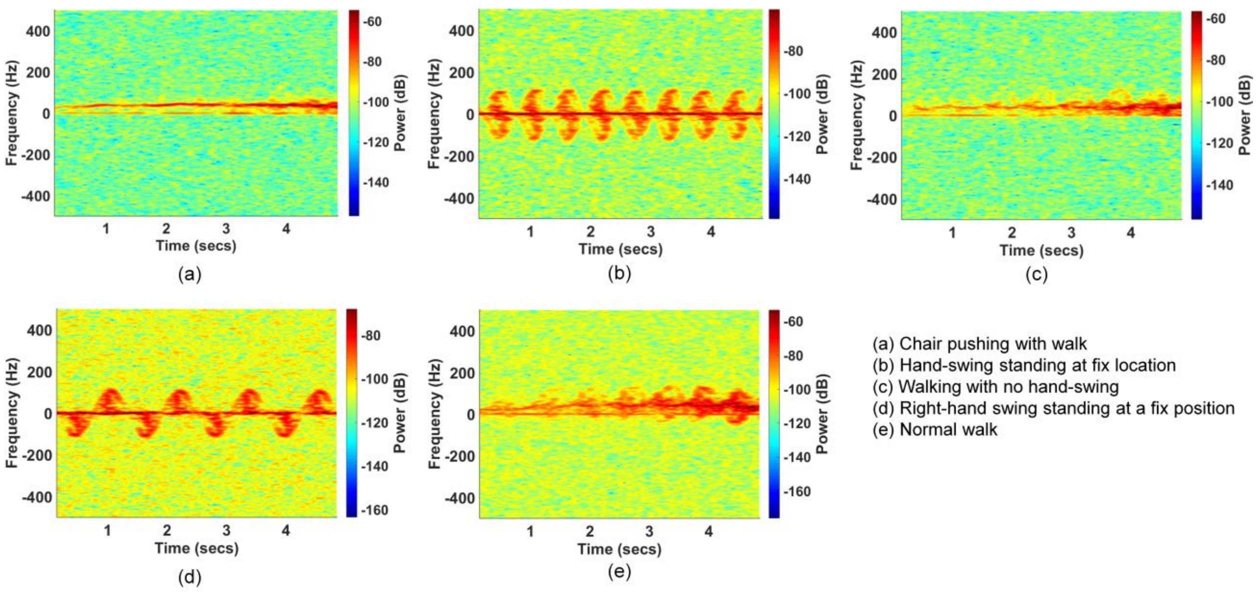


**Figure 4.5:** Generated spectrograms for one set of data from all the five experimental classes.

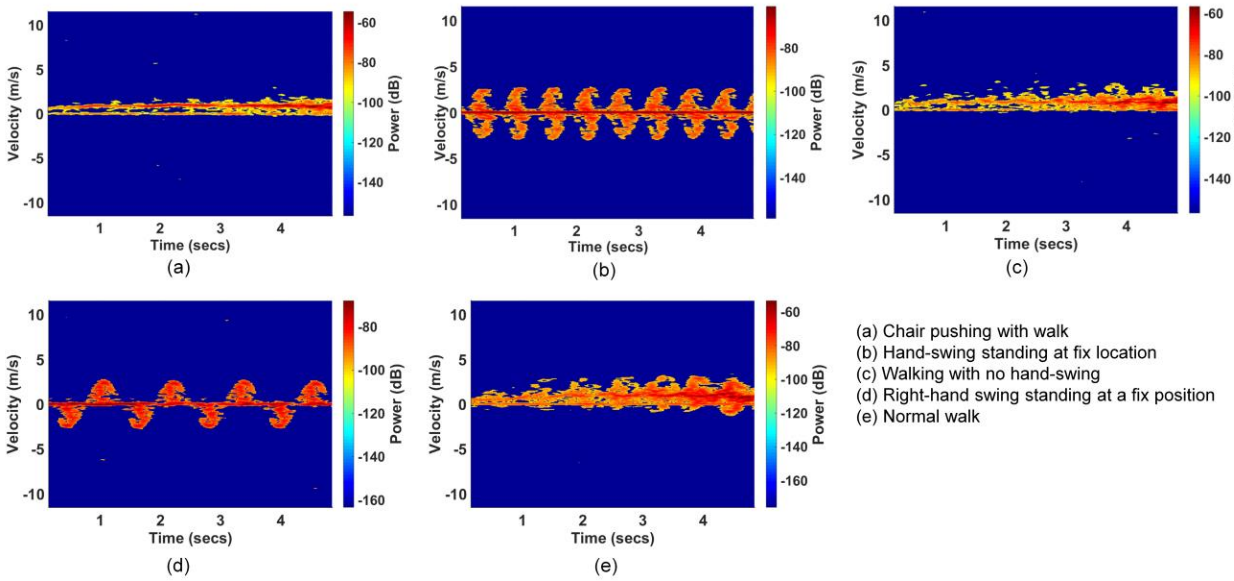


**Figure 4.6:** Background-clipped spectrogram velocity-time representation for all the human movements.

For the spectrogram's gait micro-Doppler signature highlight, thresholding is the standard method. The intensity threshold is applied here to clip out the noise in the time-frequency plane and retain the human movement associated micro-Doppler. The generated spectrogram for all five cases includes three groups of walking of human subject while the remaining two groups are associated with the human subject standing at the same place and performing some activity. Even in performing an activity, the positions of the subject were changed multiple times to make a variable data set. Since the energy received in the backscattered signal is strongly dependent on the target to antenna relative distance, a fixed threshold value cannot be applied for the fixed position activity cases. The solution to this problem was suggested by applying a spectrogram's texture statistics based threshold, which depends upon the time-frequency distributed intensity levels. For clipping out the background, a threshold limit of $K_{clip} = Mean + 1.2 \times (Standard\ deviation)$ is chosen, for highlighting micro-Doppler signatures. The enhanced micro-Doppler signatures of all the five cases corresponding to Figures 4.5(a-e) data are shown in Figures 4.6(a-e).

### 4.5.2 Features Extraction

After highlighting the spectrogram's micro-Doppler signature, the next phase is the feature extraction from the spectrogram. To make digital computation easy, the spectrogram information is converted to a grayscale image which has the intensity variation in the range 0 to 1 which are equivalent to minima and maxima values of original spectrogram's intensities. The new gray scale image intensity range (0 - 1) is quantized into $L$ = 256 levels and the other intensity values of spectrogram are mapped to only these $L$ discrete levels. The defined spatial features as mentioned previously have been computed for each gray-scaled spectrogram, which are the main input to the classifier.

The entropy variations with respect to data collected is shown in Figure 4.7(a). The spectrogram energy distribution is higher in the cases where micro motions due to structural components dominates and a larger value of entropy is expected. The given plot infers that the entropy value also depends on the frequency content spread. Its value is highest for class 2, second highest for class 5, i. e., the normal walking case and lowest for the least micro-Doppler containing case i.e., for class 1 of chair pushing case. Class 4 offers less entropy value in comparison to class 2 because the micro-Doppler frequency spread becomes half for single hand swing condition than both the hand swing case.

The mean and variance values corresponding to each experimental data number plots are shown in Figure 4.7(b). It can be observed that the values of these two features are least for class 1 where the micro-Doppler is least while bulk translation is the highest one. On the contrary, the value of these two features are highest for the data class 2 where only micro-Doppler portion occurs strongly due to the both hand swings and absence of the bulk translation related main Doppler information. For other three classes, the value of these features depends upon the contribution of micro and main Doppler motions in the backscattered signal. The third and fourth moments, i.e., skew and kurtosis based feature variation plots are illustrated in Figure 4.7(c). It can be observed that their values achieve highest for all the data belongs to class 1. The lowest values are occurring for the normal walking case, i. e., case 5. The class 3 values contain for moderate value in between class 1 and class 5.

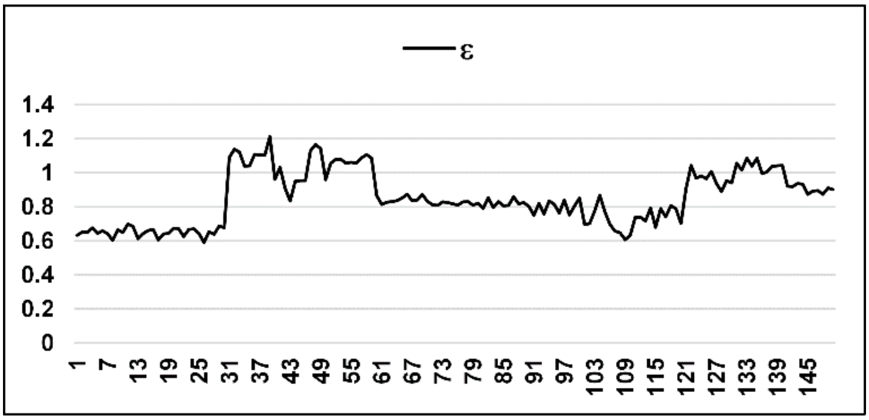


(a)

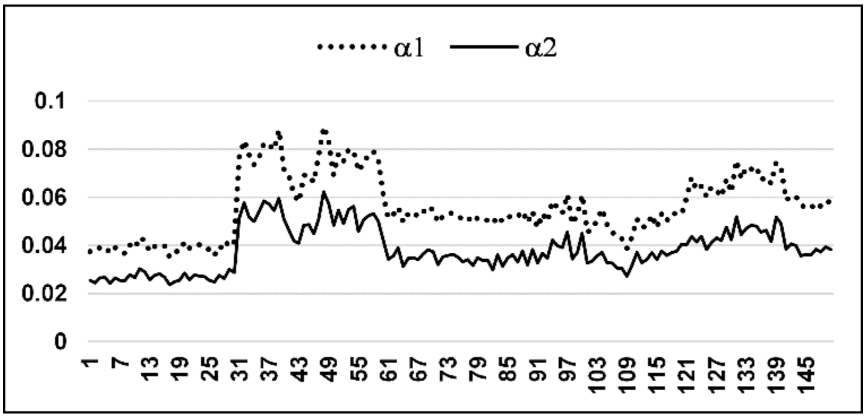


(b)

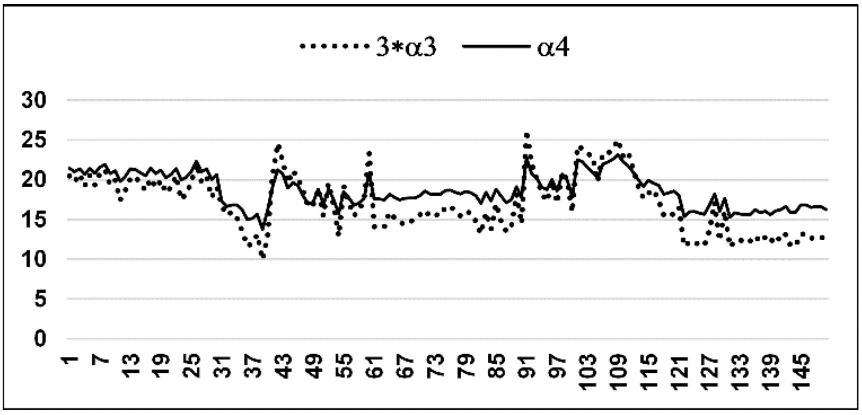


(c)

**Figure 4.7:** (a) Variation of feature 1 (entropy) with collected data; (b) Variation of feature 2 (mean) and feature 3 (variance) with collected data; (c) Variation of feature 4 (skewness) and feature 5 (kurtosis) with collected data.

### 4.5.3 Activity Classification

The classification ability of each feature is tested in terms of classification accuracy and given in Figure 4.8(a). We can observe from the chart shown as Figure 4.8(a) that the individual feature effect on the classification is highest for entropy and mean while least for the Kurtosis. The combined effect of all the features on the improvement in accuracy is also represented in Figure 4.8(b). As feature number increases during the training of the OVA SVM model, we find that the system net accuracy increases from 75.0% to 96.7%. It is evident that gradual increment in the accuracy gets saturated near the application of 5 features simultaneously.

A total of 150 data are collected for the experimentation where 30 data belongs to each class. 80% of the data for each class are used for training purpose of the model, while the rest of the 20% on the testing purpose. For five different classes, the training model is used based on one versus all (OVA) classification using SVM classifiers. In the training data, five-fold cross validation is performed which involves the $5^{th}$ portion of data randomly for the accuracy check during training phase of a classifier system. The cross validation accuracy of the system after completion of training is found to be 96.7%. The generated confusion matrix of the trained model is shown in Table 4.3. We can observe from the confusion-matrix that class 4 data is the most miss-classified as class 3 i.e. 8.3%. Class 1 (Pushing chair), class 3 (walking with no hand swing) and class 5 (normal walking) have yielded no false prediction and achieved 100% accuracy in true class prediction. Least true predication class has been observed in class 4, i.e., swinging single hand standing at different fixed positions.

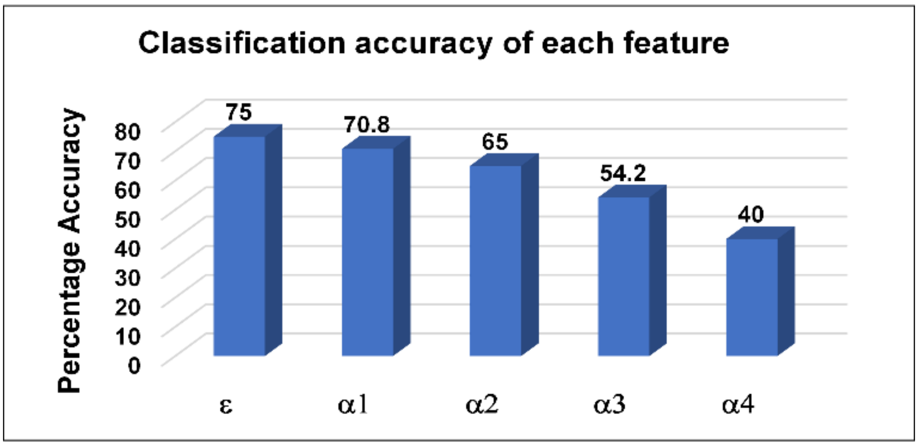


(a)

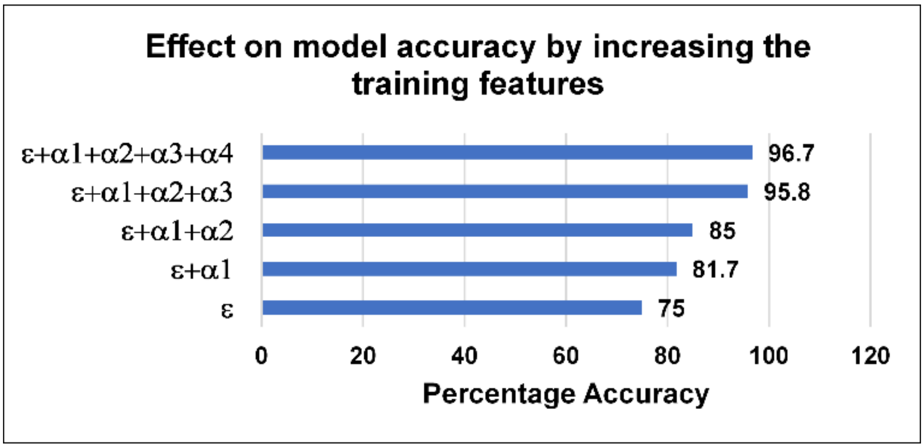


(b)

**Figure 4.8:** (a) Classification accuracy of the proposed model with individual features; (b) Training model validation accuracy with increase training features.

This least prediction accuracy is suspected due to the data collection at different locations of the subject under test while performing the activity which leads to the strong variation in the received backscattered signal. The testing accuracy of the trained model is tested using testing data sets and it is found to 93.33%. Out of 30 test input data, only 2 of them are miss-classified during prediction phase; thereby enhancing the efficiency of the system. The accuracy comparison of proposed spatial feature extraction based method is shown in Table 4.4 which indicates that the accuracy of adopted approach with least processing complexity is better and suitable for multi class classification.

**Table 4.3:** Confusion matrix.

| | | Predicted Class | | | | |
|---|---|---|---|---|---|---|
| | | Class1 | Class2 | Class 3 | Class4 | Class5 |
| True Class | Class 1 | 100% | 0.0% | 0.0% | 0.0% | 0.0% |
| | Class 2 | 0.0% | 91.7% | 0.0% | 4.2% | 4.2% |
| | Class 3 | 0.0% | 0.0% | 100% | 0.0% | 0.0% |
| | Class 4 | 0.0% | 0.0% | 8.3% | 91.7% | 0.0% |
| | Class 5 | 0.0% | 0.0% | 0.0% | 0.0% | 100% |

**Table 4.4:** Accuracy comparison.

| **Group** | **Feature Type** | **Classes** | **Validation Accuracy** | **Prediction Accuracy** |
|---|---|---|---|---|
| Kim Y., *et al*. [19] | Time Frequency | 7 | 92.8% | -- |
| Shi X., *et al*. [15] | Spatial Feature | 2 | 96.27% | -- |
| Du, Lan, *et al*. [12] | Time Frequency | 3 | 96.11 | -- |
| Proposed Method | Spatial Feature | 5 | 96.7% | 93.3% |

## 4.6 Conclusions

This chapter included the classification of human movement micro-Doppler signature, which can be generated during site security monitoring. Five different human movement activities were captured by the synthesized synchronous phased system in the laboratory. The high sampling rate time domain data is used for the generation of spectrogram using sliding time window Fourier transform. The spatial features were defined for the spectrogram images. The feature and their combination were utilized for the training and prediction using one versus rest support vector machine (SVM) classifier. The training phase of the classifier includes 80% of the total data set while rest of the remaining data are used for validation. The remaining 20% of data was used for the testing of the trained model. The work covered in *Chapter 4* improved the classification accuracy up to 96.7 % for the multiclass classification problem of human activities by using the easy spatial features of time-frequency representation of the received signal by a CW radar. The method used here utilized a one vs. all approach to tackle the multiclass classification using a binary (SVM) classifier, which also reduced the effort of defining a binary tree.